# Study of time and space correlation of delay profile components in indoor/outdoor micro-cellular communication channels

*Amidian Ali A. étudiant 3e cycle*

*Dr Michel Lecours, directeur de recherche*

*Abstract: This work is based on the study of temporal and spatial variation in Impulse Response Data for two suburban and one urban sites, where signals from a nearby outdoor transmitter are received in an indoor room at 1.44, 6.7, 14.72 GHz, and also at 22 GHz [1]. The three indoor sites are rooms located in a private house in a suburban setting, an office building in a suburban setting and an office building in a dense urban high rise building setting. The work deals specifically with the study of time and space correlation of the significant components of the received delay profiles*

*Résumé: Ce travail est basé sur l'étude des variations temporelles et spatiales de réponses impulsionnelles mesurées dans deux sites suburbains et un site urbain, où des signaux en provenance d'un transmetteur extérieur voisin sont reçus dans une pièce à 1.44, 6.7, 14.72 GHz, avec quelques mesures à 22 GHz [1]. Les trois sites d'intérieur sont situés dans une résidence de banlieue, un édifice à bureaux en milieu périphérique, et un édifice à bureaux dans un centre urbain dense. Le travail porte spécifiquement sur l'étude des corrélations temporelles et spatiales des composantes significatives des profils de délais des signaux reçus.*

## 1. Introduction

In Canada, the Communication Research Center (CRC), a federal government laboratory located in Ottawa, the Canadian Institute for Telecommunications Research (CITR), one of the federally fonded Networks of Centers of Excellence, and several industrial have collaborated to conduct, studies and measurements which are required for the modeling, design and reliable operation of LMDS (LMCS) in 27.5-28.35 GHz and 29.1-29.25 GHz and of indoor/outdoor communication channels in general. A review we have made of a number of studies indicates two cases of particular interest for our own study: 1) Temporal variability to be expected on individual subscriber links 2)Multipath dispersion characteristics of individual links within a cell.

Propagation characteristics such as time delay spread, small-scale spatial variability, and temporal variability need to be investigating in more detail to indicate limitations on the capabilities of future LMDS systems [2] as shown in figure 1.

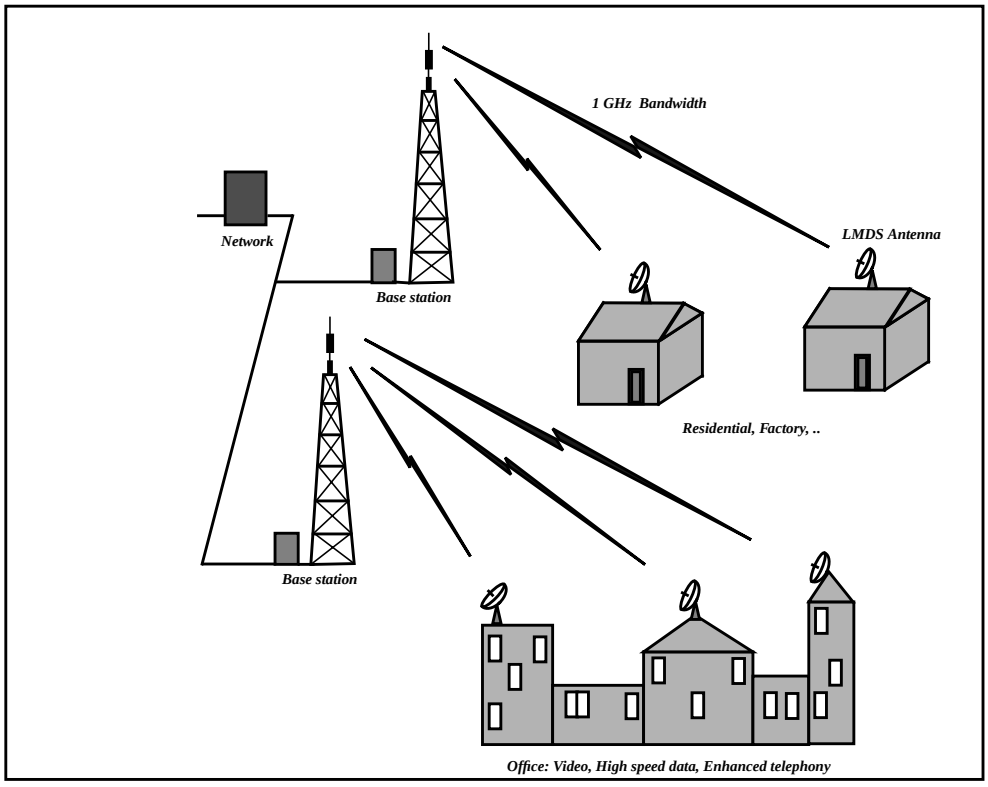


**Figure 1** :LMDS/LMCS systems

Consequently our study deals specifically with the study of time and space correlation of delay profile significant components and diversity techniques in wideband indoor/outdoor microcellular radio communication.

Our work is based on the analysis of already available CW and impulse response data for one urban and two suburban areas in the Montreal region, where signals from a nearby outdoor transmitter are received and recorded in several indoor locations, including a private house in a suburban setting, an office building in a suburban setting and an office building in a dense urban high rise setting. CW and impulse responses data where recorded at 1.44, 6.7 and 14.72 GHz. Some results are also available at 22 GHz [1] and frequency scaling may eventually be used with additional simpled propagation experiments to extend the results in frequency.

The primary focus is to obtain estimates for pertinent parameters important for wideband high data rate mobile and personal communication systems, insisting in particular on the detailed analysis of the significant multipath component in the measured delay profiles.

In particular, the time and space correlation between significant components will be computed for:

-the frequency band of operation,
-the received location within the room, and
-the different orientations of the receive antenna.

## 2. Multipath Radio Channels

Electromagnetic waves emitted from a radio transmitter will undergo a variety of treatments by the propagation medium before they reach the destination receiver. Some portion of the transmitted energy will travel along a direct imaginary line connecting the transmitted antenna to the receive antenna. Some other portions will experience such mechanisms as reflection, diffraction and scattering by structures and objects in the vicinity of the radio link. Consequently, the resultant signal detected by the receiver is in essence the sum of all individual components that arrive through different paths with different gains, phase shifts and arrival times. As the positions of either the transmitter, the receiver, or the reflecting structures change, there must also be changes in the resultant receive signal.

Further reasoning on the basis of the previously stated phenomena leads to the adoption of a linear time-varying finite-impulse response filter in modeling the lowpass equivalents of (mobile) radio channels. In such a model, a radio channel baseband equivalent is assumed to have a finite length impulse response consisting of a train of replicas of the transmitted, hypothetical, impulse waveform, i.e. the input to the linear filter. Each replica shows a unique amplitude, phase and time delay with respect to the impulse transmission time. Hence, the lowpass equivalent channel response $h(t, \tau)$ can be expressed mathematically as follows [3], [4]:

$$h(t, \tau) = \sum_{n=1}^{M(t)} a_n(t) e^{j\phi_n(t)} \delta(\tau - \tau_n(t)) \qquad (1)$$

where $M(t)$ is the time-varying number of multiple paths, while $a_n(t)$, $\phi_n(t)$ and $\tau_n(t)$ are the time-varying amplitude, phase and excess delay, respectively, of the $n^{th}$ path component, and $\delta(\cdot)$ is a Dirac delta function.

In reality, as it is impossible to generate a real impulsive waveform, pulse responses serve as approximations of the channel impulse responses in describing radio channel characteristics. With respect to the inverse of the width of the transmitted pulse, if the receiver system bandwidth is much larger than the inverse of the pulse width, the receiver will be able to resolve individual received pulses such that the equation (1) applies. This system is referred to as wideband or broadband.

It is readily seen from equation (1) that the characteristics of a radio channel vary along the axes of the observation time $\tau$ and the impulse transmission time $t$. Variations in amplitude and phase of the channel response along each of these two time axes take two separable forms:

the one caused by the variation in transmission time $t$ manifests itself in multipath fading, whereas the other, which results from the changes along the observation time $\tau$, is recognized in the form of multipath dispersion or frequency selectivity[].

The noiseless baseband output $y(t, \tau)$ from a radio channel having a lowpass equivalent channel impulse response $h(t, \tau)$ when a lowpass signal $x(t, \tau)$ modulates the transmitted signal is:

$$y(t, \tau) = h(t, \tau) \otimes x(t, \tau) = \sum_{n=1}^{M(t)} a_n(t) e^{j\phi_n(t)} \delta(\tau - \tau_n(t)) \quad (2)$$

## 3. Mathematical representation of the Impulse Response in this work

The method used to measure the impulse response over a given bandwidth consists in modulating a carrier by a "pseudo–noise sequence", (PN) thus producing a modulated BPSK type signal. In the receiver, once the demodulation is realized, one only needs to correlate the resulting signal (i.e. PN sequence modified by its passage through the channel) by an original PN sequence identical to that transmitted in order to obtain the impulse response.

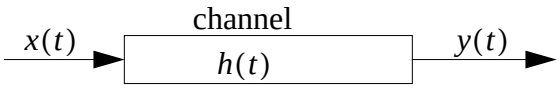


**Figure 2** : An invariant-time linear system

For our data the transmitter and the receiver were fixed, therefore, the response of the channel will be stable over a few periods. Referring to Figure (2) where $h(t)$ is the impulse response, $x(t)$ and $y(t)$ are the systems input and output, the output of the system can also be expressed in the following form [5], [6]:

$$y(t) = \int_{-\infty}^{\infty} x(t-u)h(u)du \quad (3)$$

If each side is multiplied by $x^*(t-\tau)$, then

$$y(t)x^*(t-\tau) = \int_{-\infty}^{\infty} x(t-u)x^*(t-\tau)h(u)du \quad (4)$$

Now, if $x(t)$ is a wide-sense stationary random process, the same is true for $y(t)$ [3]. E We can write:

$$R_{xy}(\tau) = R_{xx}(\tau) \otimes h(\tau) \quad (5)$$

where $R_{xy}$ and $R_{xx}$ represent cross–correlation and the auto–correlation functions respectively. If $x(t)$ has the same properties as white noise,

$$R_{xy}(\tau) = \delta(\tau) \otimes h(\tau) = h(\tau) \tag{6}$$

where $\delta(\tau)$ is the delta function. It means that the cross–correlation function $R_{xy}(\tau)$ is identical with the response of the system at time t. With regard to the system of measurement using a direct sequence spread spectrum method, a stationary random process $y(t)$ similar to white noise (flat spectrum on a large portion of the studied band) is received after its passage through the radio channel, and is correlated with a second pseudo–random process $x(t)$ identical to that transmitted signal at time $(t - \tau)$, where $\tau$ is the time of propagation of the channel. By supposing that the propagation channel is linear, the product of this cross-correlation can be regarded as a good estimated of the impulse response $h(\tau)$ of the channel [4].

## 4. Correlation Functions

Correlation functions are useful in analyzing the statistical parameters of linear systems. The correlation technique can determine the expected value of the product of two random variables, or of two random processes. The correlation will be either an auto-correlation, if the two radom variables are obtained from the same random process, or a cross-correlation, if they are obtained from different random processes [5].

The correlation functions of two random signals measure the degree of similarity between them. The cross-correlation function $R_{xy}(m)$ of two complex sequences $x(n)$ and $y(n)$ for discrete-time energy signals is obtained as follows [4]

$$R_{xy}(m) = \sum_{-\infty}^{\infty} x(n) y^*(n-m) \tag{7}$$

$$= x(m) \otimes y^*(-m), \qquad m = 0, \pm 1, \pm 2, \ldots$$

where $y^*(n)$ represents the conjugate of $y(n)$, and $'\otimes'$ denotes the discrete-time convolution operator. Some properties of this function are

* $R_{xy}(m) = R_{yx}(-m)$

* $|R_{xy}(m)| \leq \sqrt{R_{xx}(0) R_{yy}(0)}$

For a subset of power signals composed of periodic signals, the cross-correlation function as sequence becomes [4]

$$R_{xy}(m) = \frac{1}{N} \sum_{n=0}^{N-1} x(n) y((n-m))_N \tag{8}$$

$$= \frac{1}{N}[x(m) \otimes_N y(-m)], \qquad m = 0, 1, \ldots, N-1$$

where $y((n-m))_N$ denotes a circular shift operation on an N-point $y(n)$,and $'\otimes_N'$ represents an N-point circular convolution operator.

When $y(n) = x(n)$, the function becomes the auto-correlation sequence $R_{xx}(m)$ of $x(n)$.

## 5. Power Delay Profile (PDP)

The Power Delay Profile (PDP) is the magnitude squared of the measured impulse response (envelope of the received signal). It is necessary to know the total time duration, which corresponds to the number of sampling points divided by the sampling rate. In the case of the first three frequencies (i.e.: 1.44 GHz, 6.7 GHz, 14.7 GHz), 3407 points construct the time axis and the sample frequency is 100 MHz, which gives a total time duration of 34 $\mu s$. With regard to the highest frequency (22 GHz), the number total of points duration is 5110 and the sampling rate is 250 MHz, which gives a time of 20 $\mu s$. A 3D-representation of received impulse responses at different positions over a duration of 3 $\mu s$ is shown in Figure 3.

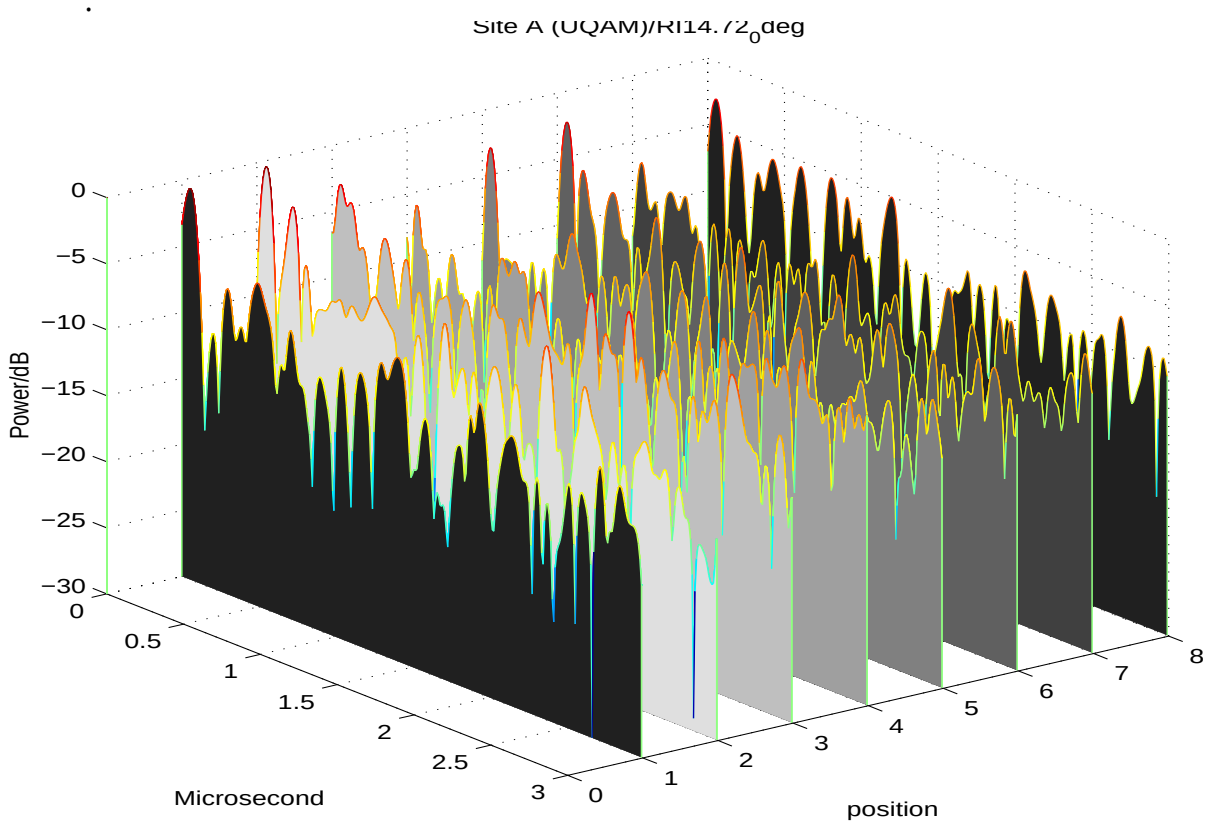


**Figure 3** : Typical 3D-variation of PDPs

## 6. Preliminary results

We used a threshold defined as Threshold = average (noise) + 4 * standard deviation (noise) [7], and in order to eliminate all contributions coming from the power from the noise, the level of the signal under this preestablished threshold value was regarded as null (as shown in figure 4). Then, each signal was swept by moving a time window (bin), comparing all data samples within each bin together (each bin contains samples). For any bin with a value larger than for the bin before and after it, we indicated a significant component of received signal.

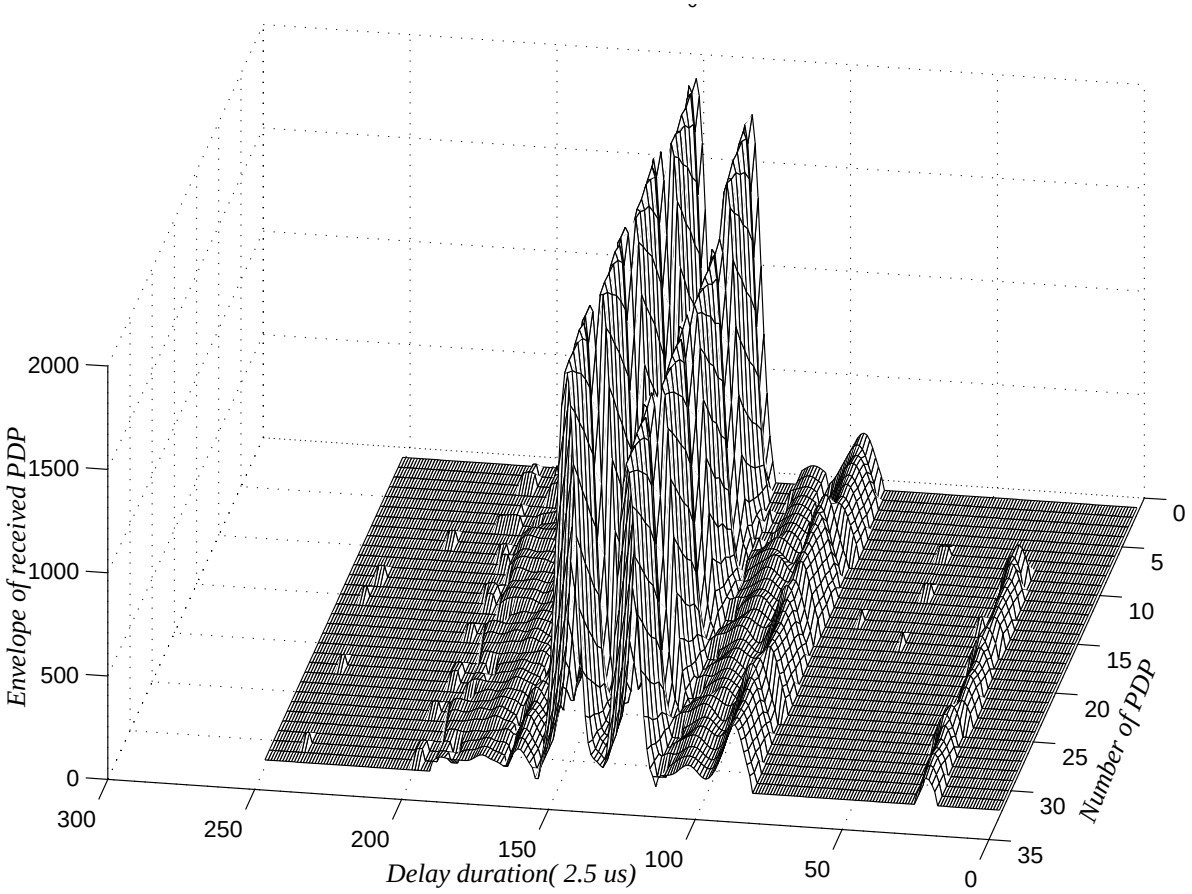


**Figure 4** : Variation of the envelope of received PDP (greater than the threshold)

In Figure 5, the variations of the peak amplitude of the eigth most significant components is shown, with the dominant component indicated as #8. Figure 5 shows the peak amplitudes relative to the dominant component.

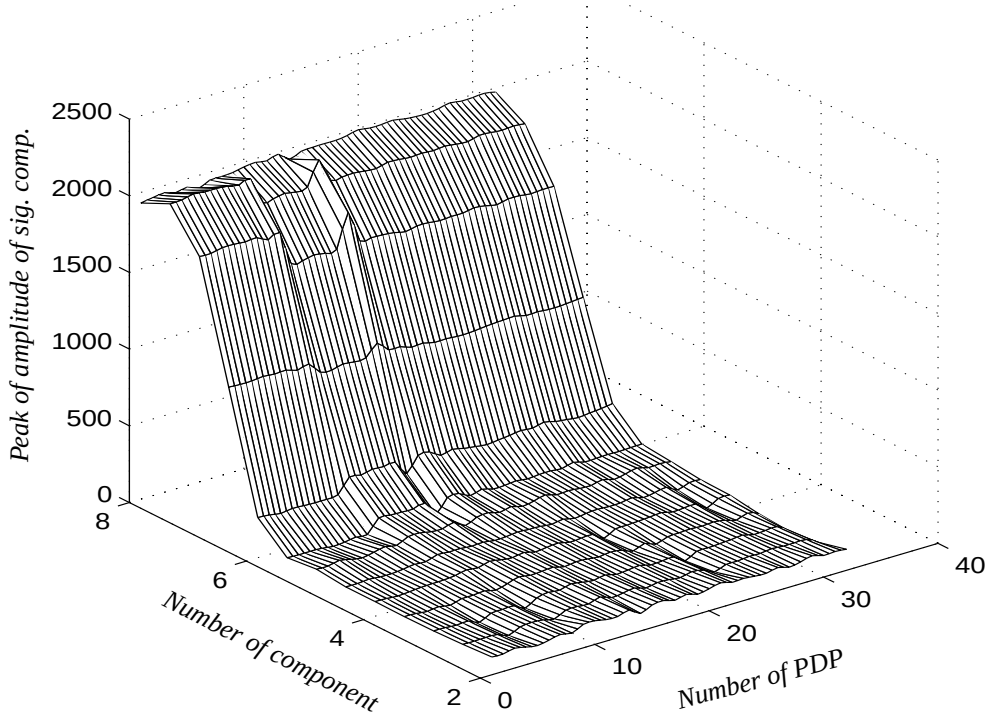


**Figure 5** : Temporal variation of significant components

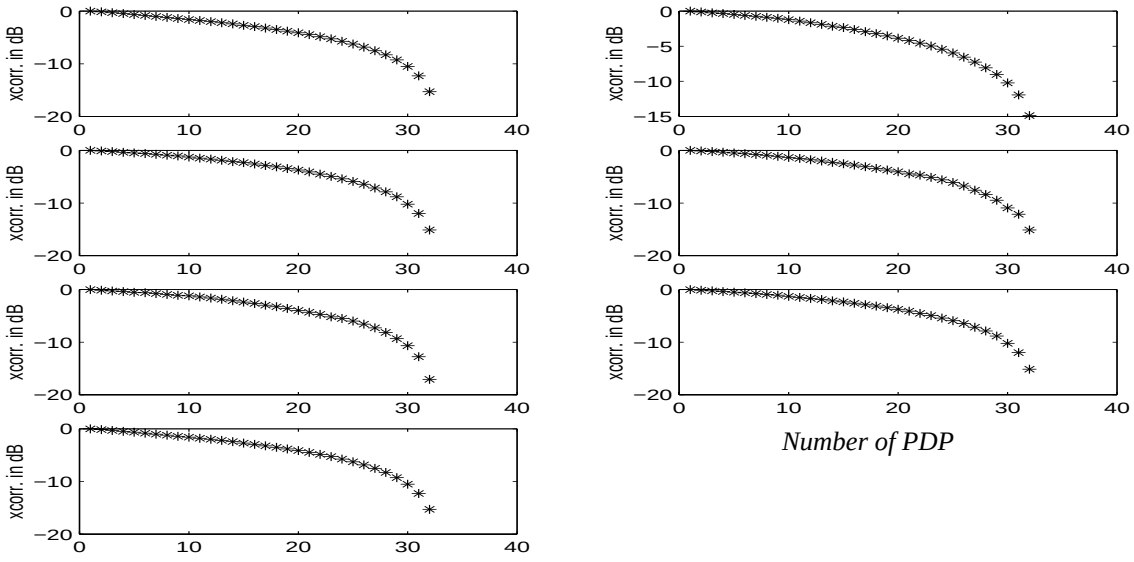


**Figure 6** : Cross-correlation of the significant components

Figure 6. represents the cross-correlation of temporal variations of different significant components. It shows how the similarity between the different significant components decreases gradually with time.

## 7. References

[1] D. Lacroix, “Caracterisation d’un canal microcellulaire urbain dans les bandes UHF et SHF”, Mémoire de mâtrise, INRS-Télécommunications, Université du Québec, Montréal, 1997.

[2] Scott V. Seidel and H. W. Arnold, ”Propagation measurements at 28 GHz to inrestigate the performance of local multipoint distribution service (LMDS),” GLOBECOM’95,Vol.1, pp. 754-757.

[3] H. Hashemi, “The indoor radio propagation channel,” Proc. of the IEEE., vol. 81, no. 7, July 1993.

[4] J. G. Proakis, Digital Communications, McGraw-Hill, 1995, ch. 2.

[5] William C. Y. Lee, Mobile Communications Engineering Theory And Applications, Second Edition, McGraw-Hill , 1997.

[6] K. S. Shanmugan, Digital and Analog Communications Systems, John Wiley & Sons, 1979, p. 415.

[7] R. J. C. Bultitude, S. A. Mahmoud, W. A. Sulliva, “Acomparison of Indoor Radio Propagation Characteristics at 910 MHz and 1.75 GHz,” in IEEE J. Selected areas Commun., vol. 7, no. 1, pp. 20-30, January 1989.